Fuzzy Variable Stiffness in Landing Phase for Jumping Robot

Juan M. Calderón, Wilfrido Moreno and Alfredo Weitzenfeld

Abstract Some important applications of humanoid robots in the nearest future are elder care, search and rescue of human victims in disaster zones and human machine interaction. Humanoid robots require a variety of motions and appropriate control strategies to accomplish those applications. This work focuses on vertical jump movements with soft landing. The principal objective is to perform soft contact allowing the displacement of the Center of Mass (CoM) in the landing phase. This is achieved by affecting the nominal value of the constant parameter P in the PID controller of the knee and ankle motors. During the vertical jump phases, computed torque control is applied. Additionally, in the landing phase, a fuzzy system is used to compute a suitable value for P, allowing the robot to reduce the impact through CoM displacement. The strategy is executed on a gait robot of three Degrees of Freedom (DoF). The effect of the impact reduction is estimated with the calculations of the CoM displacement and the impact force average during the landing phase.

1 Introduction

The development of humanoid robots has increased exponentially in the last few years. Many organizations around the world, such as RoboCup and DARPA [1], are involved in establishing guidelines for humanoid robotics development in various

J.M. Calderón (✉) · W. Moreno
Department of Electrical Engineering, University of South Florida, Tampa, FL, USA
e-mail: juancalderon@mail.usf.edu

W. Moreno
e-mail: wmoreno@usf.edu

A. Weitzenfeld
Department of Computer Science and Engineering, University of South Florida, Tampa, FL, USA
e-mail: aweitzenfeld@usf.edu

J.M. Calderón
Department of Electronic Engineering, Universidad Santo Tomás, Bogotá, Colombia

V. Snášel et al. (eds.), *Innovations in Bio-Inspired Computing and Applications*, Advances in Intelligent Systems and Computing 424,
DOI 10.1007/978-3-319-28031-8_45

application domains. The robotics road map for USA [2] and Europe has mentioned some important applications of humanoid robots. Some examples include: rescuing human victims in disaster zones, taking care of the elderly population, and any other application that involves risky actions for human beings. For these to succeed, humanoid robots need to develop advanced locomotion capabilities analogous to humans, such as walking, jumping and running. These movement capabilities are natural for humans, but they are significantly difficult for robots. Any humanoid movement requires special attention to aspects such as equilibrium, stability, soft contact, and low energy consumption. The work presented in this paper focuses on the process of vertical jumping and soft contact during the landing phase. The rest of the paper is composed of Sect. 2—Related Work, Sect. 3—Humanoid Jumping Process, Sect. 4—Model and Jumper Robot, Sect. 5—Control of Vertical Jump, Sect. 6—Experiment and Results, Sect. 7—Conclusions.

2 Related Work

The work presented in this paper extends the original ideas exposed by Kajita et al. in [3] where jumping is used as a first attempt to run, and by Raibert et al. in [4] where a study about balance and control of a legged hopping robot that is able to jump and run was presented. Additional related work includes different aspects of jumping and running models. Sakka and Yokoi explain in [5] how to use Ground Reaction Force (GRF), and robot inertia to optimize jump height using a virtual version of a HRP robot. They also propose a motion pattern generation method for vertical jumping in a humanoid robot [6]. They present a special policy of movement in the landing phase that reduces the impact force. This approach, however, does not use compliant actuators and test was performed in simulation only. A robot with compliant motor capabilities is described by Missura and Behnke [7], proposing an algorithm to generate an open-loop walking motion in a bipedal robot. While their work focused on the walking movement, they used comparable motors as in this work to generate compliant actions in the robot movements. A Fuzzy logic control approach is presented by [8–10] in a real robot called KURMET. This robot is a five-link planar biped, and it uses Unidirectional Series-Elastic Actuators (USEAs). The actuator consists of a DC brushless motor, and a planetary gearhead in series with a spiral torsion spring. This robotics platform uses a fuzzy control approach to perform jumping and running movements. Other types of actuators have been used to perform compliant movements. Such is the case of [11, 12] where they used pneumatic actuators to create an artificial muscle with similar mechanical properties to human muscles. These papers describe different features of the proposed artificial muscle, including the basic control system that is employed to develop humanoid robots with compliant movements. Similarly, [13] proposed a trajectory generation method to perform jumping and walking movements in a LUCY robot. This robot was developed using artificial pneumatic muscles as explained previously. In [14, 15] are presented studies about responsibility of gastrocnemius muscles and elastic tendons in the jumping process. The researchers evaluated the effect of muscles, tendons, and their stiffness in the height of vertical jump. These works introduced a robot dynamic model including the stiffness effect concluding that there is a dependency between the stiffness of the muscle and the ability to jump. This work focuses in the vertical jump process control and variable stiffness generation. Computed Torque Control to track the desired trajectories according to the ZMP and CoM conditions were used. The variable stiffness capability is generated without the use of any spring or dampers. All the actuators in the robot are DC Motors and the stiffness is achieved by recalculating the P and D values of the PID controller for each motor. A fuzzy system estimates the new value of P in the landing phase accordingly to the impact velocity and the desired landing displacement, i.e. soft or hard contact.

3 Humanoid Jumping Process

Vertical jumping is the action executed by human beings when the Center of Mass (CoM) is raised over the normal standup human position. This movement has to be performed solely by the muscles actions without the help of any external device. The main criteria to evaluate vertical jump efficiency is the maximum height reached in the flight phase. The vertical jump is normally divided in four phases: preparatory, take-off, flight and landing phase depicted in Fig. 1.

Preparatory Phase: When the CoM is moved to a lower position and, the potential energy decreases. The hips and knees are flexed, and the ankles are dorsiflexed [16].

Take-off Phase: When the CoM is moved to a higher position and, the potential energy increases. The hips and knees are extended, and the ankle plantars are flexed. During this phase the feet stay in contact with the ground. This phase finishes when the feet are no longer touching the ground.

Flight Phase: When the body is in the air. It starts when the feet are no longer in contact with the ground, and it finishes when they touch the ground again. The height

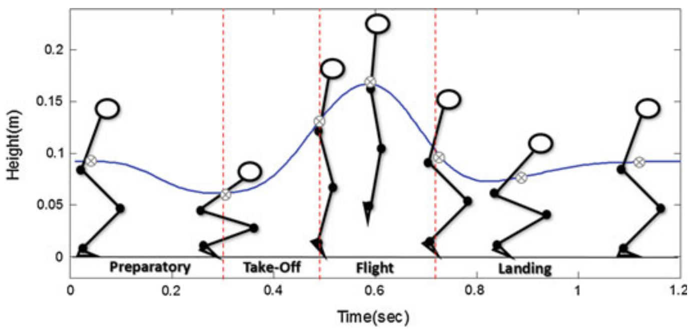

Fig. 1 Vertical jump phases and CoM trajectory

of the jump depends on the velocity reached by the CoM at the beginning of the phase. During flight, the body loses control of the rotation and trajectory, thus the position of the body is determined by the trajectory, velocity, and acceleration of the previous phase. Acceleration, velocity, position, and maximum height in the flight phase are described by (1) through (4), respectively.

$$\ddot{y}_{com}(t) = -g \tag{1}$$

$$\dot{y}_{com}(t) = -gt + V_{to} \tag{2}$$

$$y_{com}(t) = -\frac{1}{2}gt^2 + V_{to}t + y_{to} \tag{3}$$

$$y_{comMax}(t) = -\frac{V_{to}^2}{2g} \tag{4}$$

where g is gravity force, V_{to} and y_{to} are the velocity and position at the end of the take-off phase respectively.

Landing Phase: When the feet touch the ground again. In this phase the lower body tries to absorb and reduce the impact force exerted by the floor. Assuming that the robot velocity before the impact (landing velocity) is known, the impact force can be estimated as:

$$F_{i-avg} = \frac{\frac{1}{2}mV_l^2}{d} \tag{5}$$

where m is the mass of the body, V_l is the landing velocity, which can be computed using (3), and d represents the distance traveled by the object after the impact. Figure 1 shows the position of a human CoM during a vertical jump movement. The trajectory shows how the CoM is going down in the landing phase, when the legs are trying to damp the impact force exerted by the ground. A similar approach is employed by this work, where the landing impact is naturally reduced with the use of low stiffness in the electrical motors driving the ankle and knee joints.

4 Model and Jumper Robot

In the human vertical jump, both legs are doing the same movements. Using this idea, a reduced planar model with three Degrees of Freedom (DoF) is proposed. The proposed model has three joints and four links. The joints are the ankle, the knee, and the hip. The links are the foot, the shank, the thigh, and the trunk.

The kinematic model is used to calculate the position of every link, and to estimate the velocity, acceleration, and position of whole robot's CoM, as depicted in Fig. 2a. L_i denotes the length of link i, θ_i is the absolute rotation of joint i, q_i is the relative

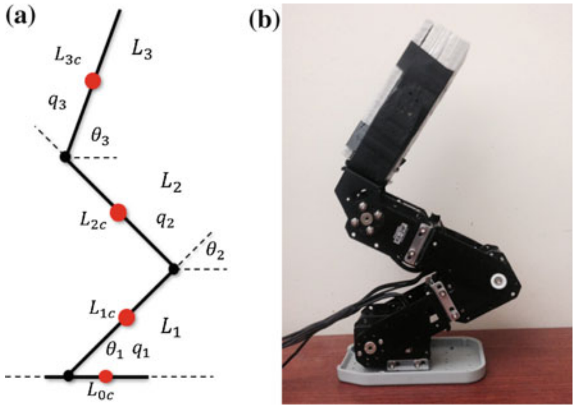

Fig. 2 Robot model and jumper robot in sagittal plane. **a** Robot Model. **b** Jumper Robot

rotation of joint i, and L_{ic} shows the position of CoM for the corresponding link i. The dynamic model is given by the Lagrange-Euler formulation as shown in (6), where $q(t) \in \mathbb{R}^n$ is the joint variable vector, $D(q)$ is a 3x3 inertial matrix, $H(q, \dot{q})$ is a 3x1 vector of Coriolis and centrifugal forces, $G(q)$ is a 3x1 gravitational forces matrix, τ represents the control torque input, and τ_d disturbance.

$$D(q)\ddot{q} + H(q, \dot{q})\dot{q} + G(q) + \tau_d = \tau \tag{6}$$

The jumper robot is a three DoF robot. The actuator of every joint is a MX-28 motor from Robotis Inc. The actuator's weight is 72 gms, and it can provide a maximum torque of 3.1 Nm. The motor runs in "endless turn" and in torque control mode. The torque control input signal can be adjusted at a 0.1 % resolution of the maximum torque allowed by the current voltage supply. The motor provides feedback about the angular position with a 0.088° resolution, the velocity, and the joint torque. Additionally, the motor has internally a micro controller unit Cortex-M3 of 32 bits, where a programmable PID controller is implemented. The Controller is implemented using a CM-2 board with an Atmega128 CPU. This board communicates with the PC via the RS232 protocol, and with the motors via the RS485 protocols. Table 1 shows the robot link parameters used in the kinematic and dynamic model.

Table 1 Parameters of robot

	Length $L_i(m)$	Mass $m_i(Kg)$	Center of mass $L_{ic}(m)$
Foot	0.010	0.051	0.045
Shank	0.098	0.051	0.072
Thing	0.098	0.051	0.072
Trunk	0.080	0.153	0.063

5 Control of Vertical Jump

5.1 Vertical Jump Conditions

Using a similar approach from Babič et al. in [17], two primary conditions to achieve vertical jump is considered. The first one, the CoM has to move upward and the displacement in the horizontal axes has to be minimum or close to zero; also, the CoM must stay into the support polygon, foot of the robot. The second one is related to ZMP [18], where the components in the horizontal axes have to be equal to zero.

The CoM position is defined by (7), where x_{com} and y_{com} are the horizontal and vertical position of the robot's CoM, m_i is the mass of the ith link, x_i and y_i are the coordinates of the CoM of the ith link.

$$x_{com} = \frac{\sum_{i=1}^{n} m_i x_i}{\sum_{i=1}^{n} m_i}, y_{com} = \frac{\sum_{i=1}^{n} m_i y_i}{\sum_{i=1}^{n} m_i} \tag{7}$$

The ZMP is defined by (8) where θ_i is the angular velocity of the ith link, and $\mathbf{I}_i$ is the inertial tensor of the ith link around the CoM.

$$x_{zmp} = \frac{\sum_{i=1}^{n} m_i x_i(\ddot{y}_i + g) - \sum_{i=1}^{n} m_i y_i \ddot{x}_i + \sum_{i=1}^{n}(\mathbf{I}_i\dot{\omega}_i + \omega_i \times \mathbf{I}_i\omega_i)}{\sum_{i=1}^{n} m_i(\ddot{y}_i + g)} \tag{8}$$

Using (7), the second derivate of x_{com} and y_{com} for control purposes can be formulated, and x_{zmp} can be computed as shown in the following equations:

$$\ddot{x}_{com} = \alpha_1\ddot{q}_1 + \alpha_2\ddot{q}_2 + \alpha_3\ddot{q}_3 + d_1 \tag{9}$$

$$\ddot{y}_{com} = \beta_1\ddot{q}_1 + \beta_2\ddot{q}_2 + \beta_3\ddot{q}_3 + d_2 \tag{10}$$

$$x_{zmp} = \gamma_1\ddot{q}_1 + \gamma_2\ddot{q}_2 + \gamma_3\ddot{q}_3 + d_3 \tag{11}$$

where α_i, β_i, γ_i, and d_i are functions of joint angles (q_i)

$$\ddot{q}_d = \begin{bmatrix} \ddot{q}_1 \\ \ddot{q}_2 \\ \ddot{q}_3 \end{bmatrix} = \begin{bmatrix} \alpha_1 & \alpha_2 & \alpha_3 \\ \beta_1 & \beta_2 & \beta_3 \\ \gamma_1 & \gamma_2 & \gamma_3 \end{bmatrix}^{-1} \left(\begin{bmatrix} \ddot{x}_{com} \\ \ddot{y}_{com} \\ 0 \end{bmatrix} - \begin{bmatrix} d_1 \\ d_2 \\ d_3 \end{bmatrix} \right) \tag{12}$$

5.2 Computed Torque Control

Computed Torque Control is a widely used control strategy based on two special approaches [19, 20]. The first one uses feedback linearization of nonlinear systems.

The second one is based on a computation of the robot's required torque by the use of the nonlinear feedback control law [21]. This kind of control is based on the concept that there is a desired tracking signal and the system tries to follow it. The main idea here is to reduce the error through a feedback linearization of the system.

The error is defined as the difference between the desired trajectory and the actual joint position as shown in equation (13), and $\dot{e}(t)$ and $\ddot{e}(t)$ can be defined using a similar equation.

$$e(t) = q_d(t) - q(t) \tag{13}$$

where $q(t)$ is the current position of the actuator (14), and it is defined from dynamic robot model given by equation (6).

$$\ddot{q} = D^{-1}(q)(H(q, \dot{q})\dot{q} + G(q) + \tau_d - \tau) \tag{14}$$

Now by back substitution (14) into (13), the second derivate of error is obtained as shown in (15)

$$\ddot{e}(t) = \ddot{q}_d(t) + D^{-1}(q)(H(q, \dot{q})\dot{q} + G(q) + \tau_d - \tau) \tag{15}$$

By defining $u(t)$ as the control input function, and $w(t)$ as the disturbance function as shown below.

$$u(t) = \ddot{q}_d(t) + D^{-1}(q)(H(q, \dot{q})\dot{q} + G(q) - \tau) \tag{16}$$

$$w(t) = D^{-1}(q)\tau_d \tag{17}$$

The feedback linearization of (16) can be inverted to yield τ as given in (18).

$$\tau = D(\ddot{q}_d(t) - u(t)) + H(q, \dot{q})\dot{q} + G(q) \tag{18}$$

where $u(t)$ is then selected as the PID feedback loop control signal,

$$u(t) = -k_v\dot{e} - k_p e - k_i\varepsilon, \quad \text{where } \dot{\varepsilon} = e \tag{19}$$

To conclude, (19) in back substitute into (18), which yield the final form for τ as shown in (20). Figure 3 depicts the Computed Torque Control schema with outer PID loop feedback.

$$\tau = D(\ddot{q}_d(t) + k_v\dot{e} + k_p e + k_i\varepsilon) + H(q, \dot{q})\dot{q} + G(q) \tag{20}$$

The Computed Torque Control is applied during all four jumping phases. The system tracks the desired trajectory $(\ddot{q}_d, \dot{q}_d, q_d)$ on the take-off phase. For the flight and landing phases, the control system tries to keep the stand-up position and reject the disturbance produced by the ground impact.

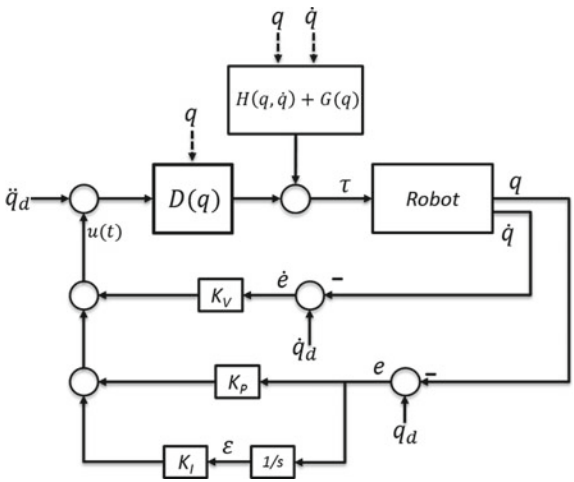

Fig. 3 Computed Torque Control schema with outer PID loop

5.3 Landing Phase with Variable Stiffness

One of the principal aims of this work is the generation of soft landing in vertical jumping movement for a real robot. The approach used to accomplish this objective is the generation of a variable stiffness in the ankle and knee joints. The stiffness capability is produced through the variation of the P gain of the PID controller. A P gain value below of the nominal designed value implies low stiffness in the motor. The D value of the PID controller is calculated assuming a critical damping response where $D = 2\sqrt{P}$.

The impact force is proportional to the squared velocity reached by the robot at contact, in accordance with (5). Based on the P gain effect on stiffness and the impact force definition given above, a fuzzy system is proposed in order to estimate the adequate P value to implement a soft contact capability.

The proposed fuzzy system is composed by two inputs and one output. The inputs are Desired-Landing and Impact-Velocity. The output is the P gain value. The fuzzy system is explained in terms of fuzzifier, set of rules and defuzzifier next.

Fuzzifier: The system has two inputs. The first one is the Desired Landing. It is relative to displacement of the center of mass from the initial landing position. This input has three membership functions called soft, medium and hard. Soft means low stiffness and it generates a large displacement. Hard means big stiffness and generates small displacement. The second input is called Impact Velocity. This variable is calculated by (2) and (3) immediately after the take-off phase using the value of the take-off velocity. This input has three memberships function called low, medium and high. Finally, the output estimates the P gain value and it is classified in three memberships called: small, medium and large. The inputs, output and P value estimation surface are shown by Fig. 4.

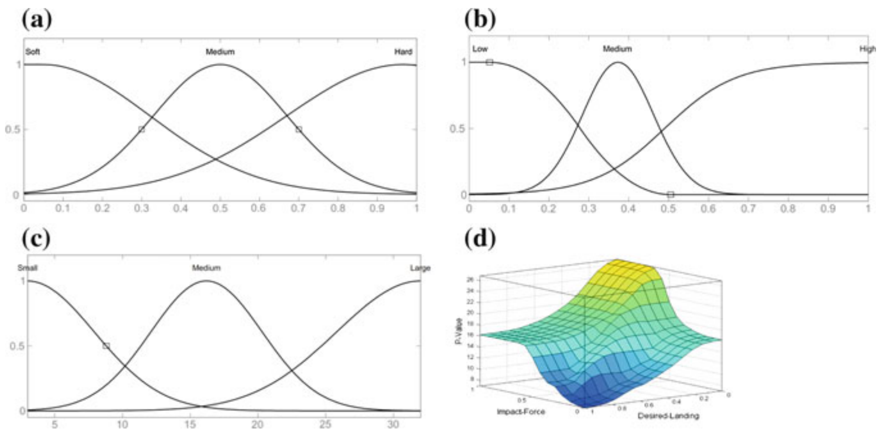

Fig. 4 Fuzzy variable stiffness estimator. **a** Desired-Landing input. **b** Impact-Velocity input. **c** P-Value output. **d** P-Value estimation surface

Table 2 Set of rules

		Impact-Velocity		
		Low	Medium	High
Desired-Landing	Soft	Medium	Medium	Large
	Medium	Small	Medium	Medium
	Hard	Small	Small	Medium

Set of rules: The set of rules are composed by nine rules that define the relation between inputs and output. This set of rules is depicted in Table 2.
Defuzzifier: The centroid is employed to estimate the final value of the P gain value.

6 Experiment and Results

In order to perform validation experiments, for vertical jumping movements in the robotics platform, the Computed Torque Control and fuzzy variable stiffness were implemented in a CM-2 board and external PC.

The experiment consists on executing several vertical jumps with different desired landing values. The objective of this experiment is to check the impact force reduction through variation of motor stiffness in the landing phase. The impact force is estimated using (5), where d is assumed as the different between touchdown position and lowest position reached by CoM in the landing phase. Large values of d, displacement in y axis of CoM in landing phase correspond to soft landing and low impact force, whereas small values of d correspond to hard landing and high impact force. Landing velocity is calculated using (3) and (4), since takeoff velocity and maximum height are known. For every attempt the inputs of the fuzzy variable stiffness system were established according to the desired landing and impact velocity estimated as previously explained. The results are shown in Figs. 5 and 6 and Table 3.

Figure 5a depicts CoM position during the whole vertical jump process. Every phase of the vertical jump is clearly recognized, especially the landing phase. The red line is the CoM position in a vertical jump with full stiffness. The blue line is

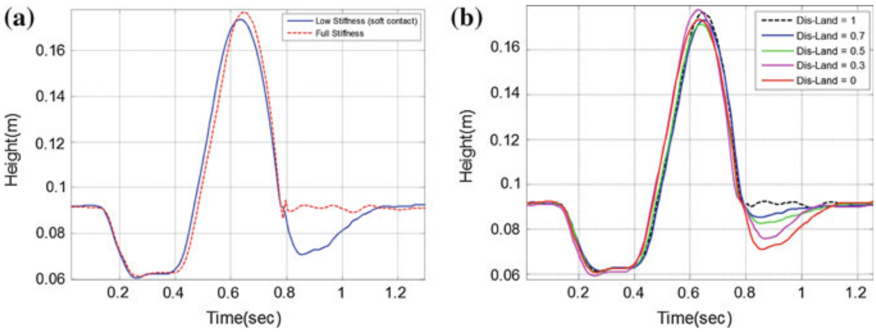

Fig. 5 Center of Mass position for different values of Disared-Landing parameter. **a** Low and full stiffness. **b** Several levels of stiffness

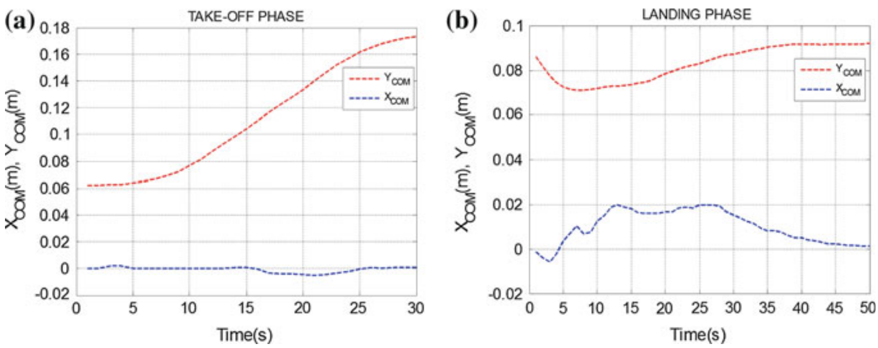

Fig. 6 X and Y position of Center of mass. **a** Take-O phase. **b** Landing phase

Table 3 Parameters of Fig. 5b

Desired-Landing	Max. high (cm)	Impact velocity (m/s)	d (cm)	Impact force average $(Kg * m/s2)$
1	2.66	1.298307	N.A.	N.A.
0.7	2.34	1.273923	0.6	41.38344
0.5	2.16	1.260041	0.855	28.40968
0.3	2.79	1.308083	1.528	17.13320
0	2.35	1.274692	2.009	12.37434

when the fuzzy stiffness system is activated and soft landing is reached. Figure 5b shows several trials with different desired landing values. According with Fig. 5b, lower values of desired landing increase the distance d, which means the impact force average was reduced. The results show impact force average, impact velocity, maximum high reached and desired landing are shown in Table 3. Table 3 shows how the impact force is reduced according to desired landing level with an impact velocity almost constant. Additionally, results show that the Computed Torque Control is allowing experiment repeatability, as the values of landing velocity and maximum height have low variance between trials. Other important aspect to analyze is the CoM displacement in takeoff and landing phases. Figure 6 shows x_{com} and y_{com} in the time for takeoff and landing phases. The maximum deviation of the CoM in the take-off phase is 0.4 cm. That means the Computed Torque Control has a good performance following the original trajectory. But in the landing phase the standard deviation of CoM is 0.75 cm and maximum deviation is 2.1 cm. Although the robot keeps balance, the movement of CoM far from the zero point can affect the robots equilibrium. We are planning to implement other control approaches such as impedance control using fuzzy estimators to improve this aspect of the landing phase.

7 Conclusions

A Fuzzy Variable Stiffness System was proposed to generate compliance capabilities in the landing phase of a jumper robot. The proposed system uses a trajectory generator based on CoM and ZMP. The control model uses a Computed Torque Control approach and the stiffness capability is generated using a fuzzy estimator. The fuzzy system estimates the P gain value of a PID controller for the landing phase allowing the displacement of the CoM from the stand up position. The estimation of the P value was done using information about Impact Velocity and Desired Landing. The proposed model was tested in a real robot having three DoF. The robot uses DC motor actuators without any dampers or springs to generate compliance capabilities. The proposed control system was evaluated running several experiments where Desired Landing was varied to get different levels of compliance. The results show a reduction of impact force according with Desired Landing where the implemented Computed Torque Control prevents the robot from falling. Different values of compliance were achieved depending on the Impact Velocity and Desired Landing values. The displacement of the x coordinate of CoM during the landing phase suggests the need for an additional control approach to improve the robot balance. Future work includes the use of compliance control with a fuzzy estimator to improve the balance of the robot.

Acknowledgments This work is funded by NSF IIS Robust Intelligence research collaboration grant #1117303 at USF and U. Arizona entitled “Investigations of the Role of Dorsal versus Ventral Place and Grid Cells during Multi-Scale Spatial Navigation in Rats and Robots”and “Octava Convocatoria Interna de Proyectos de Investigacion FODEIN 2015 # 049” at Universidad Santo Tomás, Colombia.

References

1. DARPA, DARPA Robotics Challenge, DARPA. http://www.theroboticschallenge.org/ (2015). Accessed Jan 2015
2. Georgia, I.M.I.: A Roadmap for U.S. Robotics From Internet to Robotics. Robotics in The United State of America (2013)
3. Kajita, S., Nagasaki, T., Kaneko, K.,Yokoi, K.: A hop towards running humanoid biped. In: Proceedings of ICRA'04. 2004 IEEE International Conference on Robotics and Automation (2004)
4. Raibert, M.H., Brown, B.H., Chepponis, M.: Experiments in balance with a 3D one-legged hopping machine. Int. J. Robot. Res. (1984)
5. Sakka, S., Yokoi, K.: Humanoid vertical jumping based on force feedback and inertial forces optimization. In: IEEE International Conference on Robotics and Automation (2005)
6. Sakka, S., Sian, N.E., Yokoi, K.: Motion pattern for the landing phase of a vertical jump for humanoid robots. In: International Conference on Intelligent Robots and Systems, 2006 IEEE/RSJ (2006)
7. Missura, M., Behnke, S.: Self-stable omnidirectional walking with compliant joints. In: Proceedings of 8th Workshop on Humanoid Soccer Robots, IEEE International Conference on Humanoid Robots, Atlanta, USA (2013)
8. Yiping, L., Wensing, P.M., Orin, D.E., Schmiedeler, J.P.: Fuzzy controlled hopping in a biped robot. In: International Conference on Robotics and Automation (ICRA), IEEE (2011)
9. Hester, M., Wensing, P.M., Schmiedeler, J.P., Orin, D.E.: Fuzzy control of vertical jumping with a planar biped. In: ASME 2010 International Design Engineering Technical Conferences and Computers and Information in Engineering Conference (2010)
10. Hester, M.S.: Stable Control of Jumping in a Planar Biped Robot. The Ohio State University, Ohio (2009)
11. Daerden, F.: Conception and Realization of Pleated Pneumatic Artificial Muscles and Their Use as Compliant Actuation Elements. Vrije Universiteit Brussel, Belgium (1999)
12. Beyl, P., Vanderborght, B., Van Ham, R., Van Damme, M., Versluys, R., Lefeber, D.: Compliant actuation in new robotic applications. In: NCTAM067th National Congress on Theoretical and Applied Mechanics (2006)
13. Vermeulen, J.: Trajectory Generation for Planar Hopping and Walking Robots: An Objective Parameter and Angular Momentum Approach. Vrije Universiteit Brussel, Brussel (2004)
14. Babič, J., Lenarčič, J.: Vertical jump: biomechanical analysis and simulation study, New Devel. Humanoid Robot. (2007)
15. Babič, J., Lenarčič, J.: Optimization of biarticular gastrocnemius muscle in humanoid jumping robot simulation. Int. J. Humanoid Robot. **02**, 218–234 (2006)
16. Umberger, B.: Mechanics of the vertical jump and two-joint muscles: implications for training. Strength Cond. J. **20**(5) (1998)
17. Babič, J., Damir, O., Lenarčič, J.: Balance and control of human inspired jumping robot. In: Advances in Robot Kinematics: Mechanisms and Motion (2006)
18. Vukobratović, M., Borovac, B.: Zero moment point thirty five years of its life. Int. J. Humanoid Robot. 157–173 (2004)
19. Hunt, L.R., Renjeng, S., Meyer, G.: Global transformations of nonlinear systems. IEEE Trans. Autom. Control, 2431 (1983)
20. Gilbert, E.G., Joong, H.: An approach to nonlinear feedback control with aplications to robotics. IEEE Trans. Syst. Man Cybern. 879–884 (1984)
21. Piltan, F., Hossein, M., Shamsodini, M., Mazlomian, E., Ho, A.: PUMA-560 robot manipulator position computed torque control methods using matlab/simulink and their integration into graduate nonlinear control and MATLAB courses. Int. J. Robot. Autom. 167–191 (2012)